Hazard assessment of landslide disaster using information value method and analytical hierarchy process in highly tectonic Chamba region in bosom of Himalaya

Kanwarpreet SINGH* http://orcid.org/0000-0002-7012-1815; e-mail: singhkanwarpreetnit@gmail.com

Virender KUMAR http://orcid.org/0000-0003-1881-7441; e-mail: sardavk@yahoo.com

* Corresponding author

Civil Engineering Department, National Institute of Technology, Hamirpur 177005, India

Abstract: The present study is focused on a comparative evaluation of landslide disaster using analytical hierarchy process and information value method for hazard assessment in highly tectonic Chamba region in bosom of Himalaya. During study, the information about the causative factors was generated and the landslide hazard zonation maps were delineated using Information Value Method (IV) and Analytical Hierarchy Process (AHP) using ArcGIS (ESRI). For this purpose, the study area was selected in a part of Ravi river catchment along one of the landslide prone Chamba to Bharmour road corridor of National Highway (NH-154A) in Himachal Pradesh, India. A numeral landslide triggering geo-environmental factors i.e. slope, aspect, relative relief, soil, curvature, land use and land cover (LULC), lithology, drainage density, and lineament density were selected for landslide hazard mapping based on landslide inventory. Landslide hazard zonation map was categorized namely "very high hazard, high hazard, medium hazard, low hazard, and very low hazard". The results from these two methods were validated using Area Under Curve (AUC) plots. It is found that hazard zonation map prepared using information value method and analytical hierarchy process methods possess the prediction rate of 78.87% and 75.42%, respectively. Hence, landslide hazard zonation map obtained using information value method is proposed to be more useful for the study area. These final hazard zonation maps can be used by various stakeholders like engineers and administrators for proper maintenance and smooth traffic flow between Chamba and Bharmour cities, which is the only route connecting these tourist places.

Introduction

The highway network plays very important role for socio-economic development of a nation. Landslide is a downward movement of rock mass, debris or earth which causes vulnerability of the slopes and occasional disruption of the traffic by affecting roads, buildings etc. and danger to the human life as well as flora and fauna in the hazard affected area (Cruden and Varnes 1996). Landslide hazard assessment is very essential along these roads to get desired economic benefits and safety. However, this requires a good understanding of the triggering and predisposing factors which cause landslides. Nadim et al. (2006) indicated that more

than one people per 100 km² passes away because of natural disasters in India, Colombia, Tadjiskistan, and Nepal per year. Recently on 13th august 2017, near about 48 people died during a massive landslide on Pathankot - Mandi National Highway (NH-154) in Himachal Pradesh, India where 250 meters road and two government buses have washed away because of debris flow. Many researchers have proposed bedrock geology, i.e., structure, weathering, lithology; geomorphology, i.e., slope, aspect, relative relief, curvature; soil, i.e., structure, depth, porosity, permeability; LULC and the hydrologic conditions to be the major inherent factors that influence landslides (Varnes 1984; Anbalagan 1992; Hutchinson 1995). The temporal factors like rainfall, temperature, earthquake etc. are also found to have bearing on landslide hazard zoning (Guzzetti et al. 2006; Pradhan 2010). The selection of the important causative factors in particular area is based upon the field related work, professional experience and available data. Landslide susceptibility approaches are mainly categorized namely as "qualitative, semi quantitative, and quantitative" (Guzzetti et al. 1999). The qualitative approaches are commonly expert's experience based (Aleotti and Chowdhury 1999). Weights and rates are commonly given in the semi-quantitative approaches using some logical tools such as analytical hierarchy process (AHP) (Kumar and Anabalagan 2016; Pandey et al. 2016).The quantitative statistical methods such as Weighted Linear Combination (WLC) (Anbalgan et al. 2015), Weighted Overlay Method (Sarkar et al. 1995), Fuzzy Logic (Ahmed et al. 2014), Information Value Method (IV) (Achour et al. 2017), Frequency Ratio Method (FRM) (Guru et al. 2016), Weights of Evidence (Van Westen et al. 2003; Blahut et al. 2010), Artificial Neural Network (ANN) (Pradhan and Lee 2010) and Logistic Regression Technique (LRT) (Das et al. 2010; Chen et al. 2016) were also used for landslide hazard assessment. Remote sensing (RS) and Geographical information system (GIS) techniques can play very important role for landslide hazard zonation (LHZ) by providing various datasets related to the earth surface (Guzzetti 2003; Ayalew and Yamagishi 2005). Remotely sensed data gives spatial and temporal information which is very helpful for landslide analysis, prediction, and validation. GIS methodology can provide good

alternatives to manage complex databases efficiently (Chang and Liu 2004; Mondal and Maiti 2012). Ample of literature is available in which, RS data and GIS were used for landslide inventory and hazard preparation(Gomez et al. 2000; Akbar and Ha 2011; Pourghasemi et al. 2012; Balsubramani and Kumaraswamy 2013; Sahana and Sajjad 2017).The study carried out by some of the researchers was based on GIS and remote sensing database for comparative landslide susceptibility assessment along a highway in Constantine zone of northeast Algeria using AHP and IV methods. During their study the IV method was evidenced to be relatively better than that of AHP model, with 76.59% accuracy (Achour et al. 2017). While the other researchers have shown in their study area the AHP model to be more suitable when it is compared with WLC model (Shahabi and Hashim 2015).

The present paper aimed to generate information about the causative factors affecting landslides using remote sensing and other ancillary data and to generate landslide hazard zonation maps using IV and AHP method in ArcGIS (ESRI) platform. For this purpose, the study area was selected in a part of Ravi river catchment along one of the landslide prone Chamba to Bharmour road corridor of NH-154A in Himachal Pradesh, India. Due to existence of major hydroelectricity projects on the NH-154A this route is more important. This is the single transport stretch through which a large population of this highly mountainous region survives otherwise there is no other way to go from Chamba to Bharmour. In the past, many people have lost their lives due to rock falls and sliding in this region. At various points, this route is heavily damaged because of landslides. The statistical and semi-quantitative techniques based landslide hazard assessment has never been done in literature for this highly tectonic zone in which major population is living.

1 Study Area

The methodology applied for meeting the objectives in the current study is shown in (Figure 1). First of all the study area was selected in highly mountainous region located in south-east direction of Chamba city along 62 km long NH-154A route in
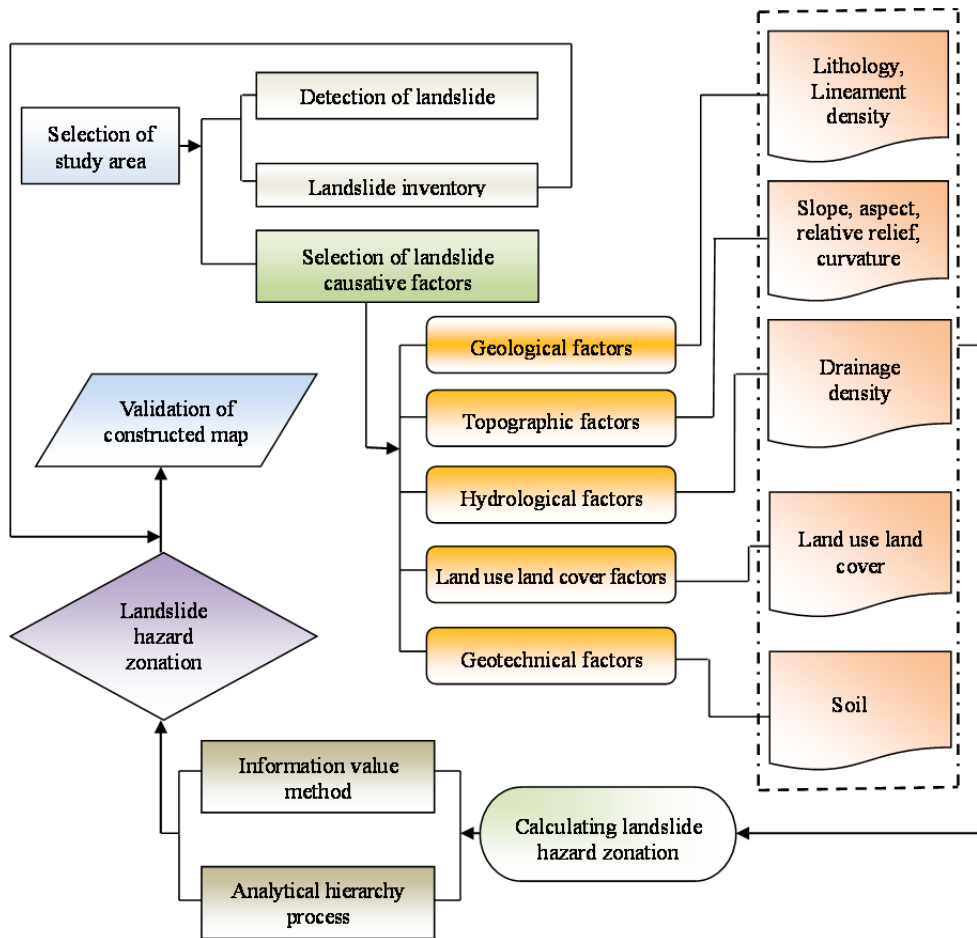
Figure 1 Flow chart showing methodology of the whole work.

Himachal Pradesh (INDIA). The starting (Chamba) and end coordinates (Bharmour) of the selected road are 32°33'12.24"N, 76°7'32.88"E and 32°26'34.08"N, 76°31'58.44"E. To delineate the study area which is about 452km², the drainage pattern along NH-154A is digitized along Ravi river flowing along the selected stretch of the road (Figure 2) using toposheets numbers i.e. 52D/2, 52D/3, 52D/6, 52D/7, 52D/10 and 52D/11, available from Survey of India (SoI). The route includes one tunnel also, which is located at Chamera III dam with the starting coordinates 32°28'15.75"N, 76°26'10.51"E and ending coordinates 32°28'21.70"N, 76°26'24.46"E. The Chamba region is highly mountainous with altitudes ranging between 2000 and 21,000 feet. The temperatures during summer season varies from "15°C (59°F) to 38°C (100°F)" and from "0°C (32°F) to 15°C (59°F)" in winter with maximum 39°C (102°F) temperature in summer and minimum −1°C (30°F) temperature in winter. The

average annual rainfall is found to be 0.79 meters for Chamba district.

1.1 Geological setting
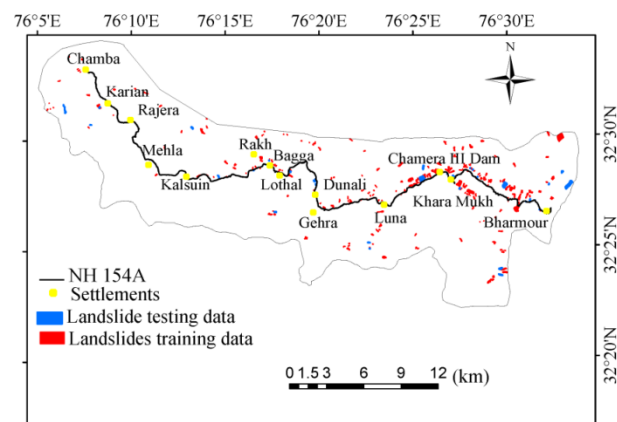
Chamba district is a wide longitudinal valley

Figure 2 Location map of the study area and mapped landslide locations.

which is located between the ranges of Zanksar in the north and Dhauladhar in the south. This is seismically active area lying in zone *V* (Amateur Seismic Centre, ASC) and the major earthquakes in Chamba were " (*M*=6.5) in 1945, (*M*=6.2) in 1947, (*M*=5.5) in 1950, (*M*=4.5) in 1995 and (*M*=4.5) in 2005 including surrounding areas of Kangra (*M* = 8) in 1905; Dharamshala (*M*=5) in 1978 and (*M*=5.7) in 1986, Kathua (*M*=5.3) in 1980" (Sharma et al. 2005). Ongoing deformations are in orogen's southern most part (Kumar and Mahajan 2001). Low lying planes to moderate and higher Himalayan mountain ranges are present in Chamba. Lesser Himalaya lies in a wide zone which is located in between the "main boundary (MBT) and main central thrust (MCT)"that runs along the base of the frontal range (Deeken et al. 2011). Large anticlines and synclines with amplitude of several kilometers are also there which represent structural features of Chamba (Frank et al. 1995). Rocks of selected area belong to Chamba formation, Katarigali formation, Batal formation, Manjir formation, Mandigrenites, Bhalai formation, and the alluvium. Their geological sequence is: (i) middle to upper proterozoic (Salkhala group), (ii) early cambrian (Haimanta group), (iii) upper proterozoic, (iv) lower cambrian to silurian, (v) lower cambrian to silurian (intrusive), (vi) recent, and (vii) quaternary. The trend of the valley is NW-SE (Wadia 1931).

1.2 Landslide inventory map

The landslide inventory map provides information about location, timing and types of landslides in a particular area. It is prepared from the historical data of individual landslide event, satellite images, field surveys, and aerial photographs (Kayastha et al. 2013). In the present research, landslides were identified by using historical records of National Highway from Public Works Department (PWD) as well as LISS III imagery and Google earth (Figure 2). With the help of hand held GPS, field reconnaissance of the landslides was confirmed and updated. A total of 322 numbers of landslides were mapped during study. The smallest landslide had an area of 74 m² while the largest one covered an area of 214,515 m². These landslides covered about 3.34 km² of the total 452 km² of study area, which is approximately 0.73% of the total area. A few of the landslide pictures were taken during field visit (Figure 3).

2 Material and Methods

The required database for the assessment of landslide hazard should be representative (Varnes 1984). It is therefore, very challenging to select the appropriate triggering factors with their contribution to landslides (Ayalew and Yamagishi 2005). Topography of surface is most important geomorphologic factor which influences the slope stability (Dai and Lee 2002). Runoff and its direction, direction of the flow, and concentration of soil moisture is controlled by topography of any area (Ayalew and Yamagishi 2005; Sujatha et al. 2012). Based on the assumption as given by some of the researchers that, the factors that control the landslides triggering in a region in the earlier period and today will also trigger landslides in the upcoming period, factors like "slope, aspect, curvature, relative relief, soil, LULC, lithology, drainage density, and lineament density", were selected in the present work (Varnes 1984; Kanungo et al. 2009). LISS-III image and Google earth were used to generate LULC and landslide inventory. In addition to this, field visits were also helpful to develop landslide inventory and land use land cover map. Cartosat - 1 DEM having spatial resolution of 30m was used to prepare slope gradient, slope aspect, curvature, and relative relief maps of the study area. Survey of India (SoI) toposheets were used to delineate drainage pattern along the road corridor. Ancillary data such as soil map and geology map were collected from various concerning departments. To rasterized all the data set, 15 m × 15 m size grid cell was used. Different type of data and its sources used in current study is mentioned in Table 1. Thematic layers of selected landslide causative factors developed from various data sources are shown in Figure 4 and 5.

2.1 Lithology

Resistance offered by the rocks towards weathering and erosion depends upon the lithology and it is very important to control the stability of slopes (Anbalagan 1992). Ground water prospects map published by NRSA, Department of Space and
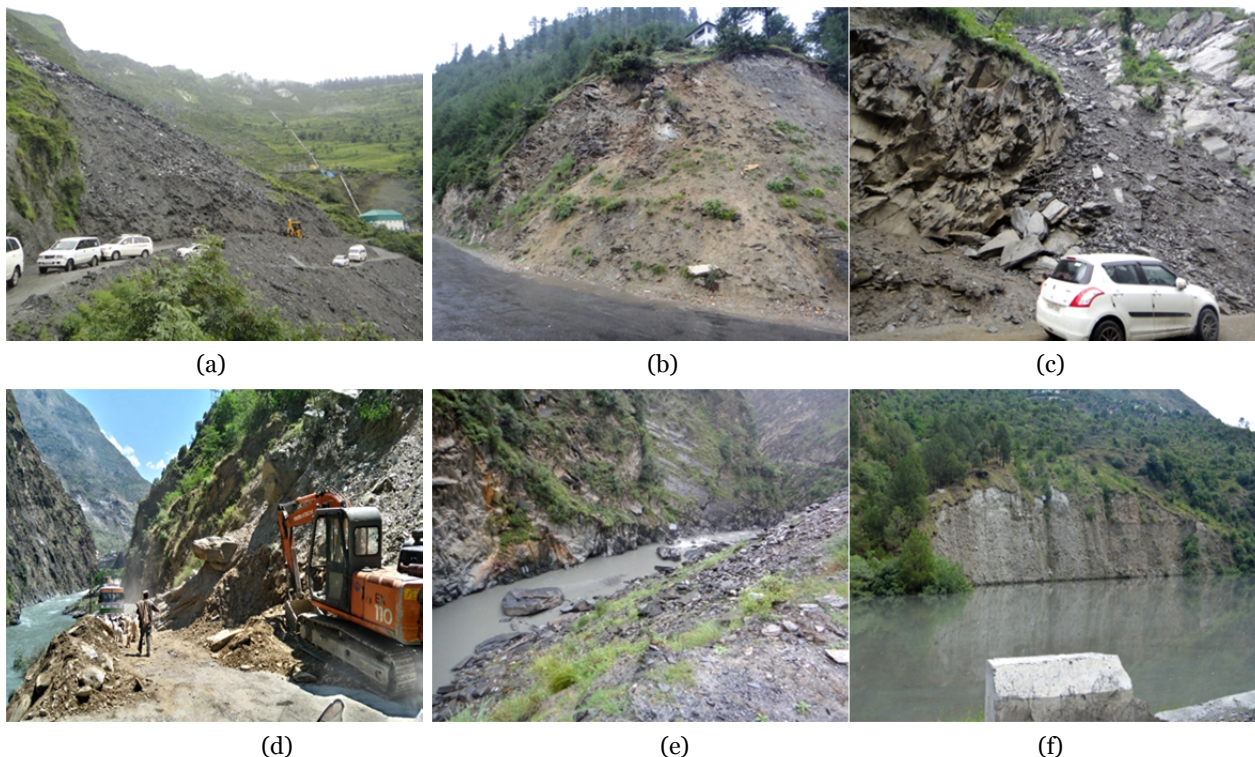
Figure 3 Field photographs of landslide types during August 2016 visit along NH - 154A showing the consequence of unplanned road construction. (a) Huge rotational failure at Trilochan Mahadev near Lothal; (b) Rock fall at Dadma showing a house at risk; (c) Debris flow blocking NH; (d) Fall near Pihura causing road blockage; (e) Boulders falling inside the river causing blockage; (f) Landslide with conglomerates falling into river at Chamera II Dam reservoir.

Table 1 Data used in present study

Data type	Source	Scale	Data derivative
Image data	LISS III		Land/use Land/cover
			Landslide Inventory
DEM	Cartosat 1		Slope
			Aspect
			Relative Relief
			Curvature
Ancillary data	Ground water prospects maps by (NRSA) Govt. of India	1: 50,000	Lineament density map
	Ground water prospects maps by (NRSA) Govt. of India	1: 50,000	Lithology map
	Soil Map of Himachal Pradesh	1: 50,000	Soil map
	Toposheets of Survey Of India (SOI)	1: 50,000	Drainage density map

Government of India, available on 1:50,000 scale were digitized to generate lithology map. Rock formation is grouped as shown in Figure 4a.

2.2 Land use and land cover

Many research studies reported the strong role of LULC for their contributions towards landslides (Lee et al. 2013). The changes in the pattern of land use, like increase in the agricultural and constructional activities, deforestation, which disturb and modify the area, are prone to landslide (Jaiswal et al. 2010). Toposheets, LISS-III satellite imagery and Google earth were used to prepare LULC map. It is, then, further categorized as mentioned in (Figure 4b). It can be found that agriculture land/populated flat land covers huge portion of selected area.

2.3 Soil

The coarse loamy, fine loamy, loamy, and loamy sand are present in Chamba district (Figure 4c). It can be noted that percentage of the coarse loamy soil is more than the other types of soil in selected study area. The Loamy soil is relatively
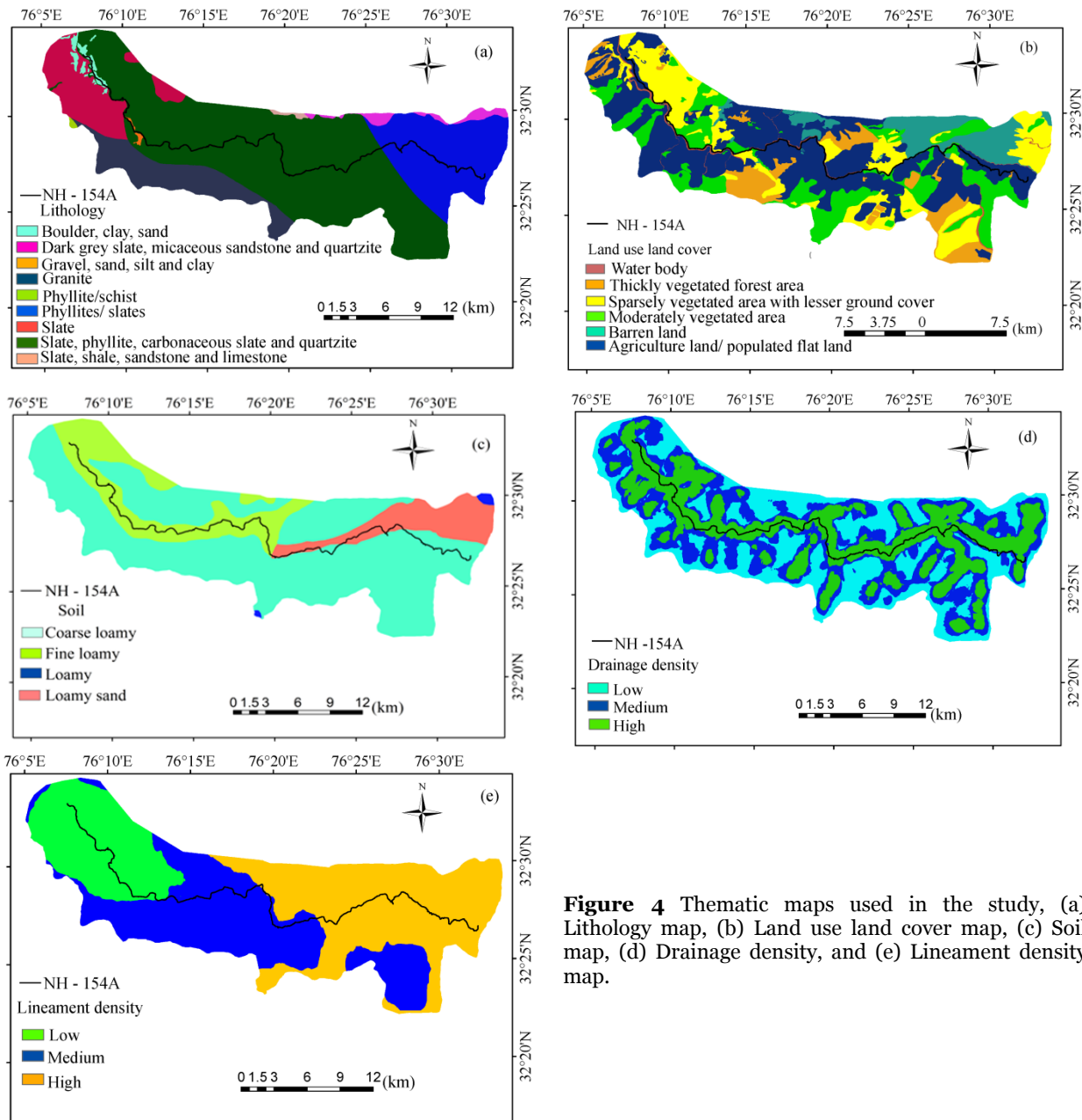
Figure 4 Thematic maps used in the study, (a) Lithology map, (b) Land use land cover map, (c) Soil map, (d) Drainage density, and (e) Lineament density map.

more prone to landslides. Quality of soil is found to vary with the relief/elevation.

2.4 Drainage density

The drainage density causes mass wasting and erosion of the slopes. For a drainage basin, drainage density is the ratio of total stream length and basin area (Demir et al. 2013). Ground water conditions also depend upon drainage density (Kavzoglu et al. 2014). Ravi river flows along the NH-154A in the study area. Many streams flowing parallel to each other joining Ravi river. The drainage pattern was digitized using toposheets and the drainage density map is prepared using focal statistics spatial analyst tool in ArcGIS (ESRI). The drainage density map is reclassified as low, medium and high classes (Figure 4d).

2.5 Lineament Density

The geological structures like fractures, faults and rock cleavages have important role to build up pore pressure (Ramakrishnan et al. 2013). Active
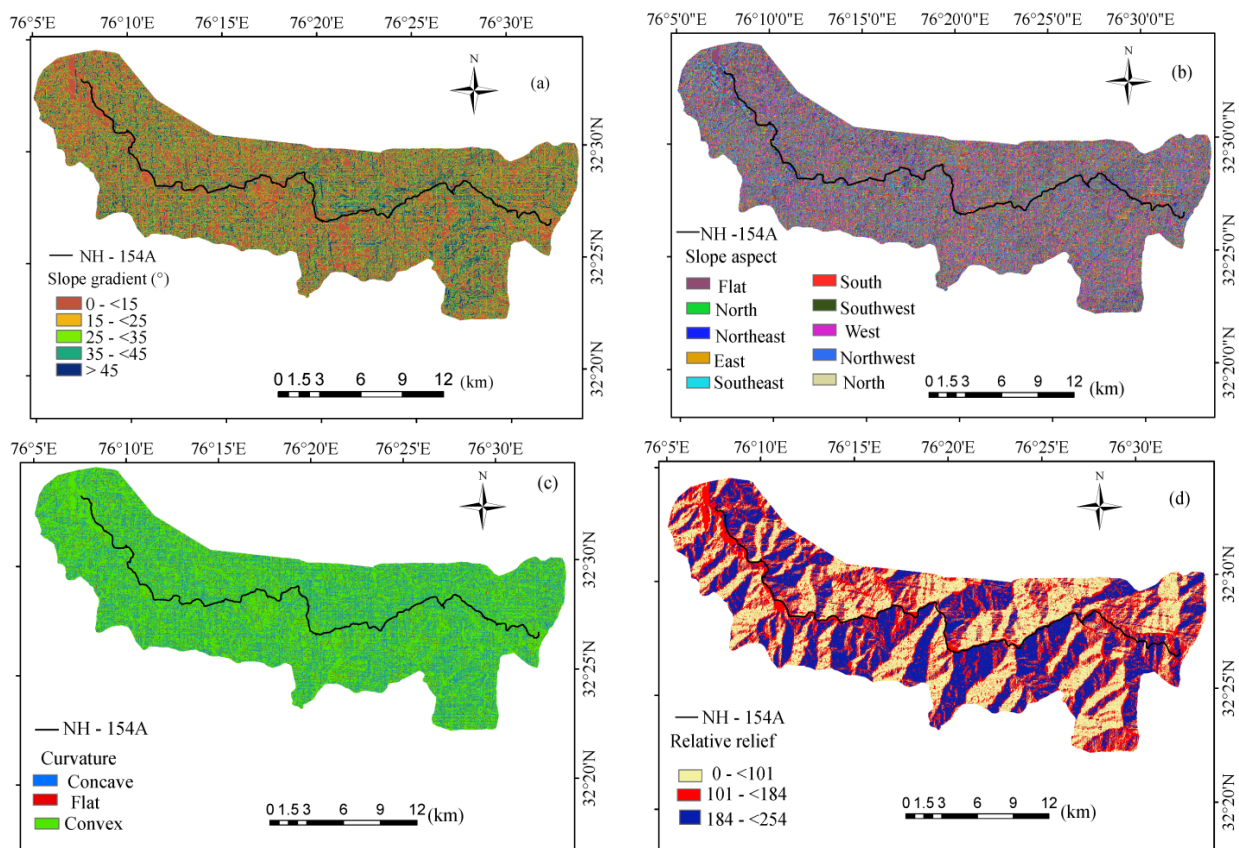
Figure 5 Various thematic maps (a) Slope gradient map (in degree), (b) Slope aspect map, (c) Slope curvature map, and (d) Relative relief map.

faults results in the increase in landslide hazard because of intense shearing (Leir et al. 2004). The published geological maps and literature data obtained from NRSA, Department of Space, Government of India, were digitized to take out lineaments. The lineament density map is derived using focal statistics tool in ArcGIS (ESRI). The lineament density map is reclassified as low, medium and high classes (Figure 4e).

2.6 Slope gradient

The slope is the rate of change of elevation in steepest fall direction. Slope gradient is a major factor for stability of a slope because of its influence on shear force (Lee and Min 2001). Slope gradient also controls the flow movement (Ercanoglu and Gokceoglu 2004). The slope map is categorized as shown in (Figure 5a).

2.7 Slope aspect

The aspect of a slope is known as the direction

of the slope facet with respect to the north. The solar heat effect, dryness of air and soil moisture is closely linked with slope aspect (Yalcin 2008). The derived slope aspect map is classified into ten classesas shown in Figure 5b.

2.8 Curvature

The curvature is the intersection of the random planes with surface (Ramesh and Anbazhagan 2015). Inflow and outflow of the water is controlled by the curvature of slope. The curvature map of the study area is classified as mentioned (Figure 5c).

2.9 Relative relief

The relative relief, which is change in the elevation, affects the natural conditions resulting in landslide occurrences. In the present work, relative relief is found to vary from 0 to 254 m. The relative relief map is classified as shown in Figure 5d.

3 Landslide Hazard Zonation Analysis

Bivariate statistical analysis (Information value method) and a semi-quantitative technique (Analytical hierarchy process) were conducted to prepare LHZ maps in ArcGIS environment in current study.

3.1 Information value method (IV)

The IV method is the invention of Yin and Yan in 1988 and later it was modified by one of the researcher named as (Van Westen in 1993). To predict an event spatially, this statistical method is useful. The IV method follows the parameters and their relation with event. It is used to calculate the weights of classes in a factor map. For an area in which landslides are induced by various causative factors having different classes, the information value can be considered as the ratio of landslides density in each factor class to landslides density in the total area.

The information value, represented in equation as Ii of each causative factor, Xi is determined as:

$$Ii = log \frac{Si/Ni}{S/N} \qquad (1)$$

where, Si=landslide pixels with the presence of causative factor Xi; Ni=pixels with causative factor Xi; S=total landslide pixels; N=total pixels in the study area.

If Ii is negative, it means less likelihood of occurrence of the landslide i.e., less effect of causative factor for landslide occurrence while the positive Ii indicates greater likelihood of occurrence and greater effect of causative factor. According to Yan (1988), if the relationship is strong then score will be higher. The total information value is obtained as:

$$I = \sum_{i=1}^{n} log \frac{S_i/N_i}{S/N} \qquad (2)$$

3.2 Analytical Hierarchy Process (AHP)

The analytical hierarchy process is an important tool to analyze and synthesize the weights of complex decisions related to different factors and their classes influencing landslides (Vargas 1990). This method is also useful for landslide hazard mapping (Feizizadeh and Blaschke 2012). The three principles - decomposition, comparative judgment and synthesis of priorities - are the base of this process. In the first step of AHP, the decision elements or causative factors are arranged in an order to show the hierarchy. Then, the pairs are compared in a matrix according to their comparison possibility and thereafter, the weights have to be given to each of the causative factor to calculate consistency ratio (CR). Saaty (1980, 1990, and 1994) gave a pair wise comparison matrix to calculate factor weight of each criterion. Scale is given to different factors on the basis of their degree of preferences such as one, three, five, seven and nine to the equal, moderate, strong, very strong and extremely strong contribution of one activity or factor over another, respectively. Intermediate scale in between 1-9, can also be given on the basis of the contribution of a factor. In the comparison matrix (pair wise), each causative factor was compared with other landslide causing factor. For every causative factor and its subclasses were also compared by assigning weights to them.

It is clearly seen in Table 2 that how the weights were assigned inside a comparison matrix to different factors in between the ranges of 1-9 on the basis of their importance. For the inverse comparison, the weight values vary in terms of the reciprocal (between 1/2 and 1/9) of the weight given to dominant causative factor. Consistency ratio (CR) is determined on the basis of an equation suggested by one of the researcher named as Saaty to check the consistency of each matrix (Saaty 1990, 1994). The CR value can be calculated as

$$CR = \frac{CI}{RI} \qquad (3)$$

where, CI is Consistency Index and RI is Random Index.

CI can be determined as:

$$CI = \frac{\lambda max - n}{n - 1} \qquad (4)$$

where, λmax = Major or principal eigen value of the matrix; n= order of matrix.

Saaty and Vargas (2000) developed reciprocal matrices using scales "1/9, 1/8, 1/7…1…8, 9". The average RI is obtained from Table 3 for different order of matrixes. For the present study, CR value obtained by considering all causative factor weights for pair wise comparison matrix comes out to be

Table 2 Weights and rates for causative factor and each subclass in a causative factor (CR=consistency ratio)

Factors comparison	(1)	(2)	(3)	(4)	(5)	(6)	(7)	(8)	(9)	(10)	Normalized Eigen weight W_k
(1) Slope gradient	1										0.0259
(2) Slope aspect	0.33	1									0.0177
(3) Relative relief	3	3	1								0.035
(4) Curvature	2	3	1	1							0.0323
(5) LULC	7	5	5	7	1						0.1114
(6) Lithology	9	7	7	9	3	1					0.1920
(7) Soil	7	9	9	7	5	2	1				0.2581
(8) Drainage density	5	5	3	5	0.33	0.2	0.2	1			0.0750
(9) Lineament density	7	9	7	7	5	2	1	5	1		0.2515
CR = 0.077											
Comparison of factor classes											w_{ik}
Slope gradient (°)											
(1) 0-<15	1										0.0335
(2) 15-<25	3	1									0.0580
(3) 25-<35	5	3	1								0.1118
(4) 35-<45	7	7	3	1							0.2523
(5) >45	9	9	9	3	1						0.5442
CR= 0.078											
Slope aspect											
(1) Flat	1										0.0432
(2) North	3	1									0.0655
(3) Northeast	0.33	0.33	1								0.0182
(4) East	0.5	0.2	2	1							0.0289
(5) Southeast	1	2	7	7	1						0.0895
(6) South	5	7	9	5	5	1					0.2423
(7) Southwest	7	3	9	5	2	0.33	1				0.1508
(8) West	0.33	0.14	1	0.33	0.11	0.11	0.11	1			0.015
(9) Northwest	1	1	5	5	1	0.2	0.2	5	1		0.0624
(10) North	9	9	7	7	5	1	3	9	9	1	0.2828
CR = 0.079											
LULC											
(1) Thickly vegetated forest area	1										0.0373
(2) Agriculture/populated flat land	3	1									0.1854
(3) Sparsely vegetated area with lesser ground cover	5	1	1								0.1438
(4) Moderately vegetated area	7	1	3	1							0.2035
(5) Barren land	9	1	5	5	1						0.3981
(6) Water body	1	0.2	0.14	0.14	0.11	1					0.0316
CR = 0.08											
Curvature											
(1) Concave	1										0.6810
(2) Flat	0.11	1									0.0688
(3) Convex	0.33	4	1								0.2500
CR = 0.002											
Drainage density											
(1) Low	1										0.0563
(2) Medium	7	1									0.2941
(3) High	9	3	1								0.6494
CR = 0.05											
Relative relief											
(1) 0 -< 101	1										0.6695
(2) 101 -< 184	0.33	1									0.2668
(3) 184 -< 254	0.11	0.2	1								0.0635
CR = 0.02											

(-To be continued-)

(-Continued-)

Table 2 Weights and rates for causative factor and each subclass in a causative factor (CR=consistency ratio)

Factors comparison	(1)	(2)	(3)	(4)	(5)	(6)	(7)	(8)	(9)	(10)	Normalized Eigen weight W_k
Soil											
(1) Coarse loamy	1										0.0903
(2) Fine loamy	0.33	1									0.0461
(3) Loamy sand	3	5	1								0.1807
(4) Loamy	9	9	7	1							0.6827
CR = 0.09											
Lithology											
(1) Slate, phyllite, carbonaceous slate and quartzite	1										0.1489
(2) Dark grey slate, micaceous sandstone and quartzite	3	1									0.2113
(3) Phyllites/ slates	0.5	0.2	1								0.1049
(4) Slate, shale, sandstone, limestone	0.33	0.14	0.33	1							0.0321
(5) Granite	0.33	0.2	0.2	1	1						0.0325
(6) Phyllite/schist	0.2	0.14	0.14	1	1	1					0.0266
(7) Slate	2	3	9	7	7	7	1				0.3320
(8) Boulder, clay, sand	0.11	0.33	0.5	3	3	3	0.14	1			0.0744
(9) Gravel, sand, silt and clay	0.33	0.2	0.2	1	1	3	0.11	0.2	1		0.0369
CR = 0.094											
Lineament density											
(1) Low	1										0.0681
(2) Medium	3	1									0.1542
(3) High	9	7	1								0.7775
CR = 0.06											

0.077. If the value of *CR* is less than 0.1, it means the consistency level is reasonable while the value more than 0.1 reveals inconsistence pair-wise comparison. Since the value of *CR* in the present study is 0.077 and it is less than 0.1, so there is good consistency in pair wise comparisons. Furthermore, to calculate the landslide hazard index (LHI), the weights are subjectively combined using Eq.5 (Tanh and De Smedt 2012).

$$LHI = \sum_{j=1}^{n} W_k \times w_{ik} \qquad (5)$$

where, W_k = Weight of the factor k; w_{ik} = Weight of subclass i in factor k; n = Total number of factors; *LHI* = Landslide hazard index.

4 Results and Discussion

To prepare the LHZ map, a total 322 number of landslides were identified in the selected area. Out of the total landslides, about 290 numbers of landslides were considered as training dataset for the purpose of modeling and 32 numbers of landslides were used as testing dataset to validate the LHZ maps. Landslide training data is used for the preparation of LHZ map using statistical

Table 3 Random Index (RI) values for different matrix orders (N)

N	1	2	3	4	5	6	7	8	9	10
RI	0	0	0.52	0.89	1.11	1.25	1.35	1.4	1.45	1.49

analysis.

4.1 Application of information value method

To execute information value method, every thematic layer is combined with the training dataset using combined tool of ArcGIS(ESRI) and the *Ii* value for all classes was determined by following the Eq. 1 and the results are shown in Table 4 in the form of weights. A gradual increase in the information value is observed till the range of the slope reached up to > 45°. The >45° class has the greater information value (0.0959) which is further followed by 35°-45°range of slope (0.0886). The lowest value was calculated for slope class0° – 15°. It can be clearly seen from this observation that occurrence of landslides is probably higher on the slopes having higher degrees. As the trend of the slope degree reduces, landslide density also become low. Action of gravity and weight of the

Table 4 Spatial relationship between each factor causing landslide and the landslide using the information value model

Causative factors	Categories	Si	Ni	Si/Ni	Landslides area (%)	Area (%)	Information value
Slope gradient	0° -< 15°	4124	815164	0.0050	33.3144	40.5424	-0.0852
	15°-< 25°	1912	320139	0.0059	15.4455	15.9222	-0.0132
	25° -< 35°	1870	288026	0.0064	15.1062	14.3250	0.0230
	35° -< 45°	2170	287370	0.0075	17.5296	14.2924	0.0886
	>45°	2303	299946	0.0076	18.6040	14.9178	0.0959
Slope aspect	Flat	482	75339	0.0063	3.8936	3.7470	0.0166
	North	997	154098	0.0064	8.05	7.6641	0.0215
	Northeast	1113	194663	0.0057	8.9910	9.6816	-0.0321
	East	1675	292501	0.0057	13.5309	14.5476	-0.0314
	Southeast	1153	189872	0.0060	9.3141	9.4433	-0.0059
	South	2060	289418	0.0071	16.6410	14.3942	0.0629
	Southwest	1259	194390	0.0064	10.1704	9.6680	0.0220
	West	1593	296161	0.0053	12.868	14.7296	-0.0586
	Northwest	1156	190658	0.0060	9.3383	9.4824	-0.0066
	North	891	133545	0.0066	7.1976	6.6418	0.0348
Relative Relief	0 -< 101	6056	674024	0.0089	48.9215	33.5227	0.1641
	101 -< 184	4278	672789	0.0063	34.5585	33.4613	0.0140
	184 -< 254	2045	663832	0.0030	16.5199	33.0158	-0.3007
Curvature	Concave	3446	455698	0.0075	27.8374	22.6642	0.0892
	Flat	508	92075	0.0055	4.1037	4.5793	-0.0476
	Convex	8425	1462872	0.0057	68.0588	72.7563	-0.0289
Drainage Density	Low	2329	670986	0.0034	18.8141	33.3716	-0.2488
	Medium	2733	670843	0.0040	22.0777	33.3645	-0.1793
	High	7317	668816	0.0109	59.1081	33.2637	0.2496
Lineament Density	Low	636	458073	0.0013	5.1377	22.7823	-0.6468
	Medium	2246	737846	0.0030	18.1436	36.7979	-0.3059
	High	9497	814726	0.0116	76.7186	40.5206	0.2772
Soil	Coarse loamy	7216	1415633	0.0050	58.2922	70.4069	-0.0820
	Fine loamy	1078	365490	0.0029	8.7082	18.1777	-0.3196
	Loamy sand	3365	221025	0.0152	27.1831	10.9927	0.3931
	Loamy	720	8497	0.0847	5.8163	0.42260	1.1387
LULC	Thickly vegetated forest area	131	185471	0.0007	1.0582	9.22445	-0.9403
	Agriculture / populated flat land	3601	805626	0.0044	29.0895	40.0680	-0.1390
	Sparsely vegetated area with lesser ground cover	3610	405242	0.0089	29.1622	20.1548	0.1604
	Moderately vegetated area	996	395417	0.0025	8.0458	19.6661	-0.3881
	Barren land	3914	191526	0.0204	31.6180	9.5256	0.5210
	Water Body	127	27363	0.0046	1.0259	1.3609	-0.1227
Lithology	Slate, phyllite, carbonaceous slate and quartzite	4927	1157898	0.0042	39.8012	57.5883	-0.1604
	Dark grey slate, micaceous sandstone and quartzite	1073	35387	0.0303	8.6679	1.7599	0.6924
	Phyllites/ slates	6076	377209	0.0161	49.0831	18.7605	0.4176
	Slate, shale, sandstone, limestone	0	5181	0	0	0.2576	0
	Granite	0	209432	0	0	10.4161	0
	Phyllite/schist	0	2309	0	0	0.1148	0
	Slate	196	197482	0.0009	1.5833	9.8218	-0.7926
	Boulder, clay, sand	107	22186	0.0048	0.8643	1.1034	-0.1060
	Gravel, sand, silt and clay	0	3561	0	0	0.1771	0

Notes: Si = landslide pixels with the presence of causative factor Xi; Ni = pixels with causative factor Xi.

loose strata will be more on the steeper slopes in comparison to the moderate slopes but if the shear strength of the material being remain same for both of the steep and moderate slopes, the steep

slope having more mobilizing force will fail early than the moderate slope. In case of the slope aspect, slopes with their faces towards the south have more information value (0.0629) followed by north (0.0215) and southwest (0.0220). Landslide occurrence is very low on the slopes having their faces towards west with -0.0586 information value. Southern aspect of the investigated zone receives excessive rainfall which makes it more prone to landslides. In terms of relative relief, class 0 -101m has more IV value of 0.1641 while very less landslides occurred in class 184 - 254m and the value is occurred as -0.300, confirming here an insignificant trend of this factor. In case of curvature, concave class (0.0892) found to be more susceptible to failure while the flatter slopes have lesser IV as -0.0476. The area where the drainage density is high, landslide occurrence is also higher (0.2496) while in low class of drainage density the IV observed as -0.2488, for which the landslide occurrence is probably low. In high drainage density terrains, stream bank erosion and toe cutting may further leads to landslides because of river and its gullies or tributaries flow.

Lineaments are the important factors which control different types of failures of slopes such as "planar, wedge, and toppling" failures. Orientation and mechanical strength of the discontinuities commonly affects the landslide triggering phenomena (Andrea et al. 2010). From the three different classes low, medium, and high of lineament density, the IV value is more for high class and observed as -0.2772 which is decreasing from medium (-0.3059) to low (-0.6468) class. Among the different types of the soils present in the study area, the highest IV value (1.1387) for landslide occurrence is found in loamy type of the soil and the slopes those have fine loamy soil are not much prone to landslides (-0.3196). Loamy type of soil is prone to the sheet erosion, gully erosion, and creep also. In the case of LULC, only thickly vegetated forest area class have lesser IV value (-0.9403) while barren land is more susceptible to landslides with information value of (0.5210). Sparsely vegetated area with lesser ground cover class also has positive IV value (0.1604) but it is lesser than barren land. In case of lithology, the various classes i.e. i) dark grey slate, micaceous sandstone, quartzite and ii) phyllites/ slates have positive information values i.e. 0.6924

and 0.4176, respectively. Finally, the calculated IV value weights are summed up by using Eq. 2 to delineate final IV method based LHZ map. The simplest form of the LHI equation which was executed using a raster calculator in map algebra tool of GIS to generate LHZ map on the basis of Eq. 2 is given as:

$$LHI_{IV} = (Ii \text{ Slope gradient}) + (Ii \text{ Slope aspect}) + (Ii \text{ Relative relief}) + (Ii \text{ Curvature}) + (Ii \text{ Drainage density}) + (Ii \text{ Lineament density}) + (Ii \text{ Soil}) + (Ii\text{LULC}) + (Ii\text{Lithology}) \quad (6)$$

The landslide hazard index for all grid cells was found to vary from -3.347 to 2.793. Based on these values, the LHZ map was categorized as "very low, low, medium, high, and very high hazard" in ArcGIS (ESRI) environment using natural break system suggested by some of the researchers (Pourghasemi et al. 2012). The results are shown in Figure 6.The distribution of study area under these categories as shown in Figure 7 which clearly shows that 15.4% portion of area under investigation falls under low hazard zone with minimum number (1.5%) of the landslides occurring in this zone. On the other hand, 11.93% of the selected area is under very high hazard zone with higher percentage of the landslides occurring in that zone. The low hazard, medium hazard and high hazard zones, those covered 29.99, 26.93, and 15.75% of the study area, respectively exhibited 9.41, 16.00 and 23.22% of the landslides. It can be noted that Bharmour and its nearby places are under high landslide hazard zone and landslide hazard is very low within the Chamba city and its nearby places.

4.2 Application of AHP method

In AHP modeling, after normalizing the weights of causative factors and their subclasses are shown in Table 2. The final average weights were calculated using arithmetic mean method. With the help of MS Excel tool, the *CI* values were calculated. *RI* values are obtained from Table 3. After this, Consistency ratio was calculated by using Eq. 3. In case of the slope as a predisposing factor triggering landslides, steeper slopes of more than 45° range have more AHP value (0.5442) as compared to the slopes which are less steep. Landslide density is higher on the north and south facing slopes with AHP value 0.2828 and 0.2423,
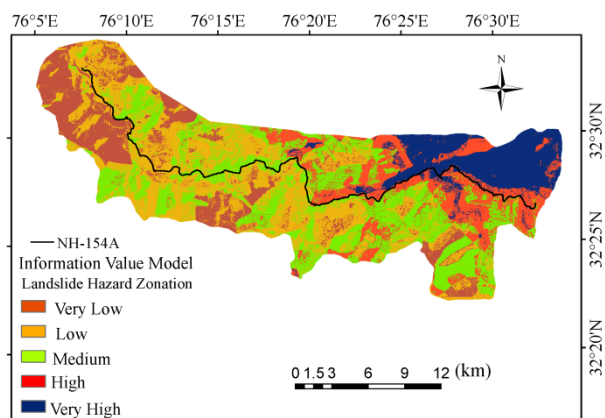
Figure 6 Landslide hazard zonation map generated using information value method.
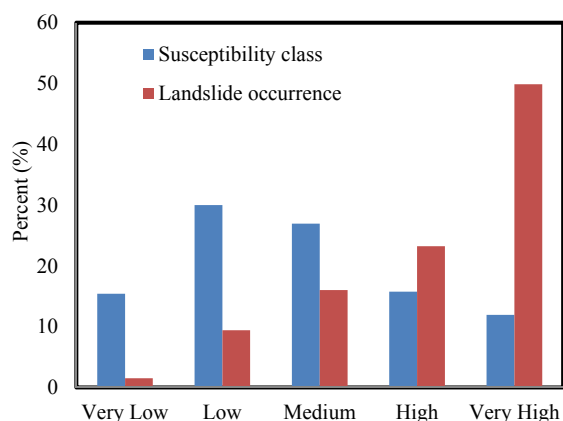
Figure 7 Landslide area percentage in the different hazard zones of the study area (Information value method).

respectively. Barren lands in current area have higher AHP value (0.3981) than the other LULC classes. Slope surface of concave type curvature is also having greater AHP value (0.6810) than that of flat (0.068) and convex (0.2500) surface. Curvature of a slope affects its saturation and erosion based on the moisture content. The areas where the drainage density is higher, the AHP have higher value (0.6494) than medium (0.2941) and low (0.0563) drainage density classes. The relative relief trend gave the AHP value as 0.6695, 0.2668 and 0.0635 for low, medium, and high relief, respectively. Loamy type of the soil is commonly more prone to landslides as compared to other types of soils present in the present research area. Lithology also affects the phenomena of landslides giving higher AHP value (0.3320) for slate unit which is more (0.2113) than the AHP value for

(dark grey slate, micaceous sandstone and quartzite) unit.

The Lineament density was also observed as a major landslide causative factor in the study area affecting landslide hazard conditions. The AHP value in case of low and medium lineament density classes in the study area was found as 0.0681 and 0.1542, respectively while the area having major discontinuities in high lineament density class have more AHP value (0.7775) than low and medium lineament density class which means that landslide occurrence is more in the area having major discontinuities like lineaments. The outcomes of the comparison of all of the landslide triggering factors showed soil as dominating factor and it is considered as a major landslide triggering factor with AHP weight 0.2581 which is more than the others.

The LHI map was delineated on the basis of Eq. 5, which was further categorized in to five subclasses as "very low, low, medium, high, and very high hazard" zones using natural break system covering about 18.67, 26.61, 14.19, 23.33, and 17.18% of the research area respectively. The simplest form of the LHI equation which was executed in GIS to delineate AHP based LHZ map on the basis of Eq. 5 that can be written as:

$$LHI_{AHP} = [(\text{Slope gradient})_{AHP} \times 0.0259] + [(\text{Slope aspect})_{AHP} \times 0.0177] + [(\text{Relative relief})_{AHP} \times 0.035] + [(\text{Curvature})_{AHP} \times 0.0323] + [(\text{LULC})_{AHP} \times 0.1114] + [(\text{Lithology})_{AHP} \times 0.1920] + [(\text{Soil})_{AHP} \times 0.2581] + [(\text{Drainage density})_{AHP} \times 0.0750] + [(\text{Lineament density})_{AHP} \times 0.2515] \quad (7)$$

The calculated LHI value for AHP model varied from 0.0713 - 0.527. From Figure 8 it can be noted that "very high hazard, high hazard, and medium hazard" zones are existing in the extreme east division (Bharmour city) of the selected investigated area while "very low hazard and low hazard" zones are lying in the west portion mostly towards main Chamba city and nearby area. It can be clearly seen from Figure 9 that 18.67% part of the investigated area exists under very low hazard zone. Both low and medium hazard zones occupied 26.60 and 14.19% of the study area, respectively. Besides, high and very high hazard zones occupied 23.33 and 17.18% of the selected area, respectively. Figure 9 showed that as the degree of hazard increases, the landslide density is also increases.

4.3 Validation of the predictive models

The landslide hazard zonation map can be verified with the help of field based information of the past landslides. In the present study, landslides in the form of rock fall, debris flows, rockslides, etc. are clearly observed in the areas of high and very high hazard zones. For assessing the overall quality of the landslide susceptibility map, the landslide density is the important factor which is to be calculated and suggested by some of the researchers (Sarkar and Kanungo 2004).

These results based on the landslide training dataset are given in Table 5 from which, an expected mismatch error can be observed showing that the very low hazard zone in case of AHP and IV models based LHZ maps covered 84.35 and 69.56 km² area with 0.0006 and 0.0005 landslides density values, respectively whereas very high hazard zones in both of the AHP and IV based LHZ maps covered 77.64 and 53.9120 km² area with 0.0192 and 0.0257 value of landslide densities, respectively. The aerial difference between the landslide covered area and landslide hazrad class covered area for both of the AHP and IV based LHZ maps can be analyzed from Table 5, because AHP is an expert experience based approach while information value method is a statistical method based on the number of pixels of landslides and landslide causative factors, due to which aerial mismatching of various hazard classes are observed in both of the LHZ maps. The existing landslide conditions in the study area are reflected in the landslide hazard zonation maps indicating high and very high hazard zones.

Several other methods are available in the literature to validate the quality of hazard zonation map(Chung and Fabbri 2003; Guzettiet al. 2006; Frattini et al. 2010). It is found that the AUC method gives better results in the prediction analysis (Fawcett 2006; Nandi and Shakoor 2009; Feizizadeh et al. 2013). The AUC method is selected
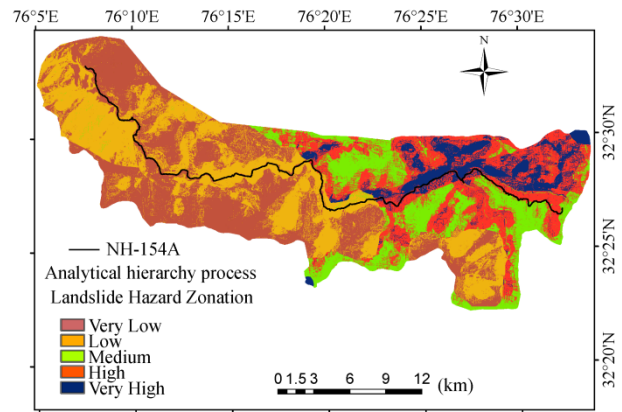

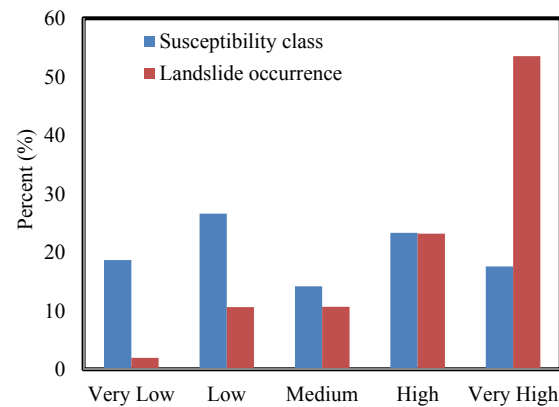**Figure 8** Landslide hazard zonation map generated using AHP method.

Figure 9 Landslide area percentage in the different hazard zones of the study area (Analytical Hierarchy Process).

to validate the results obtained from the above applied IV and AHP methods. In this method, AUC value is the base of accuracy assessment of the model. For validation process, the landslide hazard index map was classified using natural break (jenks) method in ArcGIS (ESRI). For plotting prediction rate curves, the landslide testing data were plotted against the LHI values in Microsoft Office Excel 2007. The curves give the estimation of the model fitness as per their AUC values. The AUC values were calculated using trapezium method (Kumar and Anbalagan 2016). According to Chen et al.

Table 5 Comparison of predicted landslide hazard zones and observed landslides

Hazard zones	Information value model			AHP Model		
	Area (km²)	Landslide area (km²)	Landslide density	Area(km²)	Landslide area (km²)	Landslide density
Very low	69.5691	0.0391	0.0005	84.35	0.05467	0.0006
Low	135.4882	0.2634	0.0019	120.20	0.2961	0.0024
Medium	121.6716	0.4464	0.0036	64.15	0.2976	0.0046
High	71.1326	0.6471	0.0090	105.43	0.6457	0.0061
Very high	53.9120	1.3891	0.0257	77.64	1.4910	0.0192

(2016), if AUC value lies between 0.5-1 then the model can be called as good fitted. AUC value less than 0.5 shows randomly fitted model. The AUC for landslide hazard zonation map generated using IV technique is 0.78, which shows overall 78.87% of prediction rate for LHZ map. AHP model shows 75.42% of the prediction rate. The area under curves are shown in Figure 10, which reveals that the IV model is found relatively more accurate and gave better accuracy for prediction of landslides than that of AHP model.
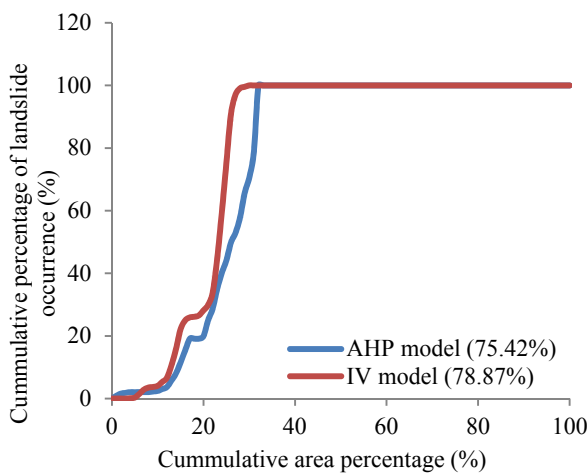
Figure 10 Prediction rate curves for the constructed landslide hazard models.

5 Conclusions

Most disastrous natural hazard in the Indian Himalaya is landslides. Hence, landslide assessment becomes imperative before the construction work of engineering projects particularly in hilly road projects such as NH-154A in Chamba district, Himachal Pradesh, India. For this purpose, information value and analytical hierarchy process models were used to generate landslide hazard zonation maps along NH-154A in Chamba district of Himachal Pradesh, India. To fulfill this objective, the landslide inventory was developed on the basis of observed landslides using different data sources. From the total 322 numbers of selected landslides, about 290 numbers of landslides (83.20%) were used as training data set for the information value model and 32 numbers of landslides (16.80%) were used as testing dataset for the purpose of validation of both of the hazard maps. Nine landslide causing factors namely "slope gradient, slope aspect, relative relief, curvature, lithology, drainage density, lineament density, soil, and land use land cover" were considered for the analysis. During modeling process, weights for each factor class were attributed. Validation of the results based on the field conditions was done by calculating landslide density in different hazard zones for both AHP and IV based hazard zonation maps. About 76% of the observed landslides from training dataset fall on high and very high hazard zones in case of AHP method which constitute 40% of the study area. In case of landslide hazard zonation map, prepared by information value method, 73% of the identified landslides from training dataset exist in high and very high hazard zones which occupied 27% of the study area. The AUC method was also applied to validate the results based on the landslides testing dataset. The AUC curves showed 78.87% prediction rate of the IV model which is higher in comparison to the analytical hierarchy process model (75.42%). Hence, landslide hazard zonation map obtained using IV method is proposed to be more useful for the study area.

References

Achour Y, Boumezbeur A, Hadji R, et al. (2017) Landslide susceptibility mapping using analytic hierarchy process and information value methods along a highway road section in Constantine, Algeria. Arabian Journal of Geosciences 10: 194. https://doi.org/10.1007/s12517-017-2980-6

Ahmed F, Rogers JD, Ismail EH (2014) A regional level preliminary landslide susceptibility study of the upper Indus river basin. European Journal of Remote Sensing 47: 343-373. https://doi.org/10.5721/EuJRS20144721

Akbar T, Ha S (2011) Landslide hazard zoning along Himalaya

Kaghan Valley of Pakistan-by integration of GPS, GIS, and remote sensing technology. Landslides 8(4): 527-540. https://doi.org/10.1007/s10346-011-0260-1

Aleotti P, Chowdhury R (1999) Landslide hazard assessment: summary review and new perspectives. Bulletin of Engineering Geology and the Environment 58(1): 21-44. https://doi.org/10.1007/s100640050066

Anbalagan R (1992) Landslide hazard evaluation and zonation mapping in mountainous terrain. Engineering geology 32(4): 269-277. https://doi.org/10.1016/0013-7952(92)90053-2

Anbalagan R, Kumar R, Lakshmanan K, et al. (2015) Landslide hazard zonation mapping using frequency ratio and fuzzy logic approach, a case study of Lachung Valley, Sikkim. Geo-Environmental Disasters 2: 6. https://doi.org/10.1186/s40677-014-0009-y.AsiaDis Stu 2:81-105

Andrea F, Andrea G, Giuseppe M (2010) Rock slopes failure susceptibility analysis: from remote sensing measurements to geographic information system raster modules. American Journal of Environmental Sciences6(6): 489-494. https://doi.org/10.3844/ajessp.2010.489.494

Ayalew L, Yamagishi H (2005) The application of GIS based logistic regression for landslide susceptibility mapping in the Kakuda-Yahiko mountains, Central Japan. Geomorphology 65(1/2): 15-31. https://doi.org/10.1016/j.geomorph.2004.06.010

Balsubramani K, Kumaraswamy K (2013) Application of geospatial technology and information value technique in landslide hazard zonation mapping: a case study of Giri Valley, Himachal Pradesh. Disaster Advances 6: 38-47.

Blahut J, VanWesten C, Sterlacchini S (2010) Analysis of landslide inventories for accurate prediction of debris-flow source areas. Geomorphology 119 (1/2): 36-51. https://doi.org/10.1016/j.geomorph.2010.02.017

Chang K, Liu J (2004) Geo-Imagery Bridging continents. Landslide features interpreted by neural network method using a high resolution satellite image and digital topographical data. Proceedings of 20th ISPRS Congress, Istambul.

Chen W, Chai H, Zhao Z, et al. (2016) Landslide susceptibility mapping based on GIS and support vector machine models for the Qianyang County, China. Environment Earth Sciences 75(6): 1-13. https://doi.org/10.1007/s12665-015-5093-0

Chung CJF and Fabbri AG (2003) Validation of spatial prediction models for landslide hazard mapping. Natural Hazards 30(3): 451-472. https://doi.org/10.1023/B:NHAZ.0000007172.62651.2b

Cruden DM, Varnes DJ (1996) Landslide types and processes, special report, Transportation Research Board, National Academy of Sciences 247: 36-75.

Dai FC, Lee CF (2002) Landslide characteristics and slope instability modeling using GIS, Lantau Island, Hong Kong. Geomorphology 42(3): 213-228. https://doi.org/10.1016/S0169-555X(01)00087-3

Das I, Sahoo S, Van Westen C, et al. (2010) Landslide susceptibility assessment using logistic regression and its comparison with a rock mass classification system, along a road section in the northern Himalayas (India). Geomorphology 114(4): 627-637. https://doi.org/10.1016/j.geomorph.2009.09.023

Deeken A, Thiede RC, Sobel ER, et al. (2011) Exhumational variability within the Himalaya of northwest India. Earth and Planetary Science Letters 305: 103-114. https://doi.org/10.1016/j.epsl.2011.02.045

Demir G, Aytekin M, Akgun A, et al. (2013) A comparison of landslide susceptibility mapping of the eastern part of the North Anatolian Fault Zone (Turkey) by likelihood-frequency ratio and analytic hierarchy process methods. Natural Hazards 65: 1481-1506. https://doi.org/10.1007/s11069-012-0418-8

Ercanoglu M, Gokceoglu C (2004) Use of fuzzy relations to produce landslide susceptibility map of a landslide prone area (West Black Sea Region, Turkey). Engineering Geology 75: 229-250.https://doi.org/10.1016/j.enggeo.2004.06.001

Fawcett T (2006) An introduction to ROC analysis. Pattern Recognition Letters27: 861-874. https://doi.org/10.1016/j.patrec.2005.10.010

Feizizadeh B, Blaschke T (2012) GIS-multicriteria decision analysis for landslide susceptibility mapping: comparing three methods for the Urmia lake basin, Iran. Natural Hazards 65: 2105-2128. https://doi.org/10.1007/s11069-012-0463-3

Feizizadeh B, Blaschke T, Nazmfar H, et al. (2013) Landslide susceptibility mapping for the Urmia Lake basin, Iran: a multi-criteria evaluation approach using GIS. International Journal of Environmental Research 7(2): 319-3336.

Frank W, Grasemann B, Guntli P, et al. (1995) Geological map of the Kishtwar-Chamba-Kulu region (NW Himalaya India). Jahrbuch Der Geologischen Bundesanstalt 138 (2): 299-308.

Frattini P, Crosta G, Carrara A (2010) Techniques for evaluating the performance of landslide susceptibility models. Engineering Geology 111: 62-72. https://doi.org/10.1016/j.enggeo.2009.12.004

Gomez H, Bradshow R, Mather P (2000) Monitoring the distribution of shallow landslide prone areas using Remote Sensing, DTM and GIS - a case study from the tropical Andes of Venezuela. In: Casanova E (ed) Remote Sensing in 21st century: Economic and Environmental applications. Balkema, Rotterndam. pp 395-401.

Guru B, Veerappan R, Mangminlen T (2016) Landslide susceptibility zonation mapping using frequency ratio and fuzzy gamma operator models in part of NH-39, Manipur, India. Natural Hazards 84: 465-488. https://doi.org/10.1007/s11069-016-2434-6

Guzzetti F (2003) Landslide Hazard Assessment and Risk Evaluation: Limits and Perspectives. In Proceedings of the 4th EGS Plinius Conference held at Mallorca, Spain. University de les IllesBalears, Spain. pp 1-4.

Guzzetti F, Carrara A, Cardinali M, et al. (1999) Landslide hazard evaluation: a review of current techniques and their application in a multi-scale study, Central Italy. Geomorphology 31(1): 181-216. https://doi.org/10.1016/S0169-555X(99)00078-1

Guzzetti F, Reichenbach P, Ardizzone M, et al. (2006) Estimating the quality of landslides susceptibility models. Geomorphology 81: 166-184.https://doi.org/10.1016/j.geomorph.2006.04.007

Hutchinson JN (1995) Landslide hazard assessment. In: Proc VI Int. Symp on Landslides, Christchurch,Vol. 1. pp 1805-1842

Jaiswal P, Van Westen CJ, Jetten V (2010) Quantitative landslide hazard assessment along a transportation corridor in southern India.Engineering Geology 116: 236-250. https://doi.org/10.1016/j.enggeo.2010.09.005

Kanungo DP, Arora MK, Sarkar S, et al. (2009) Landslide Susceptibility Zonation (LSZ) Mapping - A Review. Journal of South Asia Disaster Studies 2(1): 81-105.

Kavzoglu T, Sahin EK, Colkesen I (2014) Landslide susceptibility mapping using GIS-based multi-criteria decision analysis, support vector machines, and logistic regression. Landslides 11: 425-439. https://doi.org/10.1007/s10346-013-0391-7

Kayastha P, Dhital MR, DeSmedt F (2013) Application of the analytical hierarchy process (AHP) for landslide susceptibility mapping: a case study from the Tinau watershed, west Nepal. Computers & Geosciences 52: 398-408. https://doi.org/10.1016/j.cageo.2012.11.003

Kumar R, Anbalagan R (2016) Landslide susceptibility mapping using analytical hierarchy process (AHP) in Tehri Reservoir Rim Region, Uttarakhand. Journal Geological Society of India 87(3): 271-286.https://doi.org/10.1007/s12594-016-0395-8

Kumar S, Mahajan AK (2001) Seismotectonics of the Kangra region north Himalaya. Tectonophysics 331(4):359-371

Lee S, Min K (2001) Statistical analysis of landslide susceptibility at Yongin, Korea. Environmental Geology 40(9): 1095-1113.

Lee S, Hwang J, Park I (2013) Application of data-driven evidential belief functions to landslide susceptibility mapping in Jinbu, Korea. Catena 100: 15-30. https://doi.org/10.1016/

j.catena.2012.07.014

Leir M, Michell A, Ramsay S (2004) Regional landslide hazard susceptibility mapping for pipelines in British Columbia. Geo-engineering for the society and its environment. In: 57th Canadian geotechnical conference and the 5th joint CGS-IAH conference. pp 1-9.

MondalS, Maiti R (2012) Landslide susceptibility analysis of Shiv-Khola Watershed, Darjiling; a remote sensing and GIS based Analytic Hierarchy Process. Journal of Indian Society of Remote Sensing 3: 483-496.

Nadim F, Kjekstad O, Peduzzi P, et al. (2006) Global landslide and avalanche hotspots. Landslides 3: 159-173. https://doi.org/10.1007/s10346-006-0036-1

Nandi A and Shakoor A (2009) A GIS-based landslide susceptibility evaluation using bivariate and multivariate statistical analyses. Engineering Geology 110: 11-20. https://doi.org/10.1016/j.enggeo.2009.10.001

Pandey DD, Singh KP, Sarda VK (2016) GIS based inventory study of landslide hazard zonation in LahaulSpiti Valley between Rohtang to Baralacha La, Himachal Pradesh, India. International Journal of Earth Sciences and Engineering 09: 2847-2854.

Pourghasemi HR, Pradhan B, Gokceoglu C (2012) Application of fuzzy logic and analytical hierarchy process (AHP) to landslide susceptibility mapping at Haraz watershed, Iran. Natural Hazards 63(2): 965-996

Pradhan B (2010) Application of an advanced fuzzy logic model for landslide susceptibility analysis.International Journal of Computational Intelligence Systems 3(3): 370-381.

Pradhan B, Lee S (2010) Delineation of landslide hazard areas on Penang Island, Malaysia, by using frequency ratio, logistic regression, and artificial neural network models. Environmental Earth Sciences 60: 1037-1054. https://doi.org/10.1007/s12665-009-0245-8

Ramakrishnan D, Singh TN, Verma AK, et al. (2013) Soft computing and GIS for landslide susceptibility assessment in Tawaghat area, Kumaon Himalaya, India. Natural Hazards 65: 315-330. https://doi.org/10.1007/s11069-012-0365-4

Ramesh V, Anbazhagan S (2015) Landslide susceptibility assessment along Kohli hills Ghat road section India using frequency ratio, relative effect and fuzzy logic models. Environmental Earth Sciences 73(12): 8009-8021. https://doi.org/10.1007/s12665-014-3954-6

Saaty TL (1980) The Analytic Hierarchy Process (New York: McGraw Hill. International, Translated to Russian, Portuguese, and Chinese, Revised editions, Paperback.

Saaty TL (1990) An exposition of the AHP in reply to the paper "remarks on the analytic hierarchy process. Management Science 36 (3): 259-268.

Saaty TL (1994) Highlights and critical points in the theory and application of the analytic hierarchy process. European Journal of Operational Research 74 (3): 426-447.

Saaty TL, Vargas LG (2000) Models, Methods, Concepts and Applications of the Analytic Hierarchy Process. Boston: Kluwer Academic Publisher.

Sahana M, Sajjad HJ (2017) Evaluating effectiveness offrequency ratio, fuzzy logic and logistic regression models in assessing landslide susceptibility: a case from Rudraprayag district, India. Journal of Mountain Science 14(11): 2150. https://doi.org/10.1007/s11629-017-4404-1

Sarkar S, Kanungo D, Mehrotra G (1995) Landslide hazard zonation: a case study of Garhwal Himalaya, India. Mountain Research and Development 15: 301-309.

Sarkar S, Kanungo DP (2004) An integrated approach for landslide susceptibility mapping using remote sensing and GIS. Photogrammetric Engineering & Remote Sensing70(5): 617-625.

Shahabi H, Hashim M (2015) Landslide susceptibility mapping using GIS-based statistical models and Remote sensing data in tropical environment. Scientific reports 5: 9899. https://doi.org/10.1038/srep09899

Sharma VK, Kumar H, Kumar P (2005) Macro-seismic investigation of Chamba earthquake of 14th April, 2005, Himachal Pradesh. Geol. Surv. India, Unpublished Report, FS 2004-2005.

Sujatha ER, Rajamanickam GV, Kumaravel P (2012) Landslide susceptibility analysis using probablistic certainty factor approach: a case study on Tevankarai stream watershed, India. Journal of earth system science121(5): 1337-1350. https://doi.org/10.1007/s12040-012-0230-6

Thanh LN, De Smedt F (2012) Application of an analytical hierarchical process approach for landslide susceptibility mapping in a Luoi district, ThuaThien Hue Province, Vietnam. Environmental Earth Sciences 66(7): 1739-1752. https://doi.org/10.1007/s12665-011-1397-x

Van Westen CJ, Rengers N, Soeters R (2003) Use of geomorphological information in indirect landslide susceptibility assessment. Natural Hazards 30(3): 399-419. https://doi.org/10.1023/B:NHAZ.0000007097.42735.9e

VanWesten CJ (1993) Application of geographic information systems to landslide hazard zonation.ITC Publication, vol. 15.International Institute for Aerospace and Earth Resources Survey, Enschede. p 245.

Vargas LG (1990) An overview of the analytic hierarchy process and its applications. European Journal of Operational Research1(48): 2-8.

Varnes DJ (1984) Landslide Hazard Zonation: A Review of Principles and Practice. United Nations Educational, Scientific and Cultural Organization. p 63.

Wadia DN (1931) Thesyntaxes of the north-west Himalya-its rocks, tectonics, and orogeny.Records of the Geological Survey of India 65: 189-220.

Yalcin A (2008) GIS-based landslide susceptibility mapping using analytical hierarchy process and bivariate statistics in Ardesen (Turkey): comparisons of results and confirmations. Catena 72: 1-12. https://doi.org/10.1016/j.catena.2007.01.003

Yan TZ (1988) Recent advances of quantitative prognoses of landslide in China. In: Proceedings of the fifth international symposium on landslides, Lausanne, Switzerland. Vol. 2. pp 1263-1268.

Yin KL, Yan TZ (1988) Statistical prediction model for slope instability of metamorphosed rocks. In: Bonnard C (ed.) Proc., Fifth International Symposium in Landslides, Lausanne, Vol. 2. A.A. Balkema, Rotterdam. pp 1269-1272.